International Journal of Mechanical, Industrial and Aerospace Sciences
ISSN: 2517-9950
Vol:9, No:6, 2015

Optimal Trajectories for Highly Automated Driving

Christian Rathgeber, Franz Winkler, Xiaoyu Kang, Steffen Müller

***Abstract*—**In this contribution two approaches for calculating optimal trajectories for highly automated vehicles are presented and compared. The first one is based on a non-linear vehicle model, used for evaluation. The second one is based on a simplified model and can be implemented on a current ECU. In usual driving situations both approaches show very similar results.

***Keywords*—**Trajectory planning, direct method, indirect method, highly automated driving.

I. Introduction

IN recent years advanced driver assistance systems (ADAS) have prevailed more and more in the vehicle. Initially it was mainly longitudinal guidance systems or parking systems. More recently, lateral vehicle guidance systems using electronic power steering (EPS) have been introduced into market. Thereby functions like lane-keeping assistance or even highly automated driving can be implemented.

To ensure a safe operating, an exact planning of the vehicle's movement trajectory is necessary which explicitly account for the time t. For this purpose (nonlinear) optimization algorithms, based on the direct optimization, offer itself perfectly. These algorithms are usually used for Model Predictive Control (MPC), see for example [1], [2] or [3].

The limited computing power of current automotive ECUs however prohibits the use of non-linear optimization methods. Moreover, the proof of convergence is often difficult.

Therefore the nonlinear optimization algorithms are used for evaluation within this work. In order to be implemented on an automotive ECU, an algorithm based on a simplified vehicle model is derived, using the indirect optimization method. The approach is likewise to [4] where the problem is solved using the indirect method by the usage of polynomials in a discrete solution space. It has the advantage of being realizable on a automotive ECU and convergence is guaranteed.

In this contribution both algorithms will be compared with representative maneuvers.

After an overview on related work in Section II, the used vehicle model is presented in Section III. In Section IV we describe the optimization restrictions. Section V presents the direct optimization-based approach and Section VI the indirect optimization approach. Both approaches are compared and the differences are outlined in Section VII. In Section VIII finally a short summary is given.

Christian Rathgeber is with BMW AG, 80937 Munich, Germany (e-mail: christian.rathgeber@bmw.de)
Xiaoyu Kang is with BMW AG, 80937 Munich, Germany (e-mail: xiaoyu.kang@bmw.de)
Franz Winkler is with BMW AG, 80937 Munich, Germany (e-mail: franz.winkler@bmw.de)
Steffen Müller is with Technical University of Berlin, 13355 Berlin, Germany (e-mail: steffen.mueller@tu-berlin.de)

II. Vehicle Model

For describing the vehicle movement the well-known single-track model (STM) is used [5]. The yaw rate $\dot{\psi}$, the slip angle β and the vehicle velocity v represent the state variables:

$$\mathbf{x}_{STM}^T = \left[\dot{\psi}\, \beta\, v\right] \tag{1}$$

Its dynamics $\dot{\mathbf{x}}_{STM} = f(x_{STM}, u_{STM})$ are described in the Appendix. Usually the steering angle δ and the front and rear wheel torques T_{wf} and T_{wr} are used as an input. In our case however low-level controller generate these quantities. The steering controller uses a desired curvature κ_d the vehicle should follow as an input

$$\delta = G_\delta(s)\, \kappa_d \tag{2}$$

generating a steering angle (see for example [6]). The low-level longitudinal controller generates the front and rear wheel torques from a desired longitudinal acceleration a_d

$$T_{w,f} + T_{w,r} = G_l(s)\, a_d. \tag{3}$$

For the sake of simplicity, both transfer functions are treated as having a PT_1-behavior.

The vehicle movement in world coordinates x_w and y_w (see Fig. 1) is given by

$$\dot{x}_w = v \cos\theta \tag{4}$$

$$\dot{y}_w = v \sin\theta, \tag{5}$$

with the course angle

$$\theta = \psi + \beta. \tag{6}$$

Often one is not interested in the vehicle's position in world coordinates, but the position relative to a given lane. Thus, d_r describes the distance to the lane and θ_v the differential angle between the vehicle movement and the tangent to the lane. The lane itself is described by its curvature κ_s.

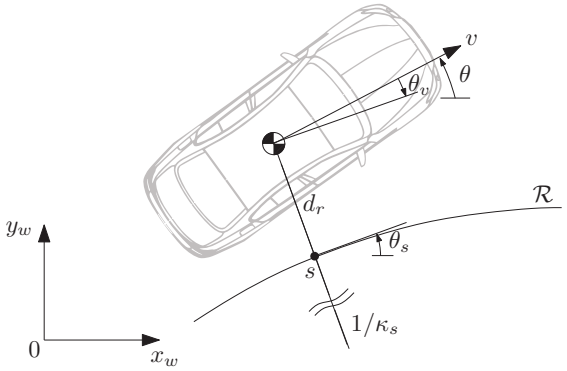

Fig. 1. Vehicle relative to a road $\mathcal{R}$ in world coordinates (x_w, y_w)

III. Optimization Restrictions

The vehicle motion is subject to various restrictions. The given actuators have saturations and the wheels are limited in traction. Moreover the freedom from collision with predicted object trajectories must be guaranteed any time. Each restriction is described in the next section.

A. Actuator Limits and Kamm's Circle

The built in EPS is saturated due to the allowed torque. This results in a saturation of the desired curvature

$$u_1 \in [\kappa_{d,min}, \kappa_{d,max}] \tag{7}$$

and its derivative

$$\dot{u}_1 \in [\dot{\kappa}_{d,min}, \dot{\kappa}_{d,max}]\,. \tag{8}$$

To consider limited traction of the tire, the relations of the so-called *Kamm's circle* are taken into account. This idealized relationship between longitudinal and lateral forces at the wheel of a vehicle allows an estimation of the attainable lateral and longitudinal accelerations [7]:

$$a_x^2 + a_y^2 \leq (\mu\, g)^2 \tag{9}$$

with the friction coefficient μ. In addition, due to the maximum

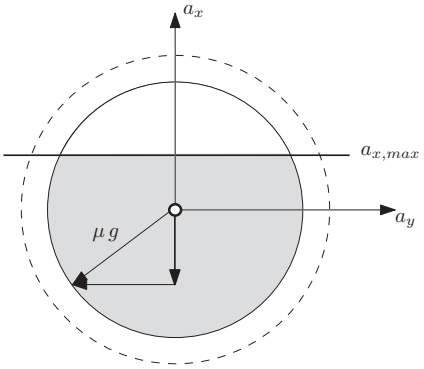

Fig. 2. Kamm's circle with restrictions on the maximum longitudinal acceleration and the traction potential

engine torque the longitudinal acceleration is limited to

$$u_2 = a_d \leq a_{x,max}. \tag{10}$$

Fig. 2 shows the resulting ellipse approximation of the combined lateral and longitudinal traction potential.

B. Collision Check

In addition to the actuator saturations and dynamic driving limits, the freedom from collision with other road users must be guaranteed. As shown in [8] the penalization of collisions can be implemented directly in the non-linear optimization algorithm. For the indirect method based approach (see Section VI) a separate collision check for each trajectory is necessary. For this a variety of efficient approaches exists: Mostly they can be divided in continuous approaches where no sampling of the trajectory in the time domain is necessary (for example [9] and [10]) and discrete-time methods where the trajectories are sampled in the time domain (for example [11]).

IV. Direct Optimization Approach

The direct optimization approach is based on the vehicle model presented in Section III. It is represented in state-space representation $f(\mathbf{x}(t), \mathbf{u}(t))$. The state-space vector and input vector are given as

$$\mathbf{x} = \left[\dot{\psi}\, \beta\, v\, \psi\, \omega_f\, \omega_r\, x_w\, y_w\right]^T \text{ and } \mathbf{u} = \left[\dot{\kappa}_d\, \dot{a}_d\right]^T. \tag{11}$$

ω_f and ω_r corresponds to the wheel speeds. As a virtual input the derivatives of the real system inputs κ_d and a_d are defined. The optimization objective is formulated as the minimization of a cost function. The resulting maneuver should be characterized by maximum comfort, thus the jerk is considered in the cost function. The lateral and longitudinal jerk represent the derivatives of the system inputs. As a second part deviations from a reference state at the end of the maneuver are penalized:

$$J = \int_0^{t_{hor}} \left(k_{j1}(\dot{\kappa}_d)^2 + k_{j2}(\dot{a}_d)^2\right) dt + k_v \left(v_{ref} - v(t_{hor})\right)^2 + k_d \left(d_{ref} - d(t_{hor})\right)^2 \tag{12}$$

The reference is given as a velocity v_{ref} in longitudinal direction and lateral offset to the given lane d_{ref}. With k_{j1}, k_{j2}, k_d and k_v the characteristics of the trajectory can be shaped. The optimization is formulated as a standard optimization problem [12]:

$$\arg\min_{\mathbf{x},\mathbf{u}} J(\mathbf{x}(t), \mathbf{u}(t)) \tag{13}$$

subject to

$$\dot{\mathbf{x}}(t) = f(\mathbf{x}(t), \mathbf{u}(t)), \mathbf{x}(t_0) = \mathbf{x}_0 \tag{14}$$

$$g(\mathbf{x}(t_{hor})) = 0 \tag{15}$$

$$h(\mathbf{x}(t), \mathbf{u}(t), t) \leq 0 \tag{16}$$

A direct multiple-shooting approach [13] will be used with a prediction horizon of t_{hor}, divided in N subintervals: the model dynamics are discretized on a uniform time grid $t_0, ..., t_N$ by numerical integration over the time intervals $[t_j, t_{j+1}]$. The inequality constraints are discretized on the same time grid. The control input $\mathbf{u}$ however is discretized as piecewise constant $\mathbf{u}_0, ..., \mathbf{u}_{N-1}$ over the time intervals. The discretization is done using Euler's method. With $g(\mathbf{x}(t_{hor}))$ it is ensured that the vehicle is parallel to the lane at the end of the maneuver ($\theta_v = 0$). The other restrictions (see Section IV) are formulated as inequality constraints ($h(\mathbf{x}(t), \mathbf{u}(t), t)$). For the multiple-shooting method, the continuity of the state trajectory must be requested in addition as a boundary condition ($\mathbf{x}(t_{j+1}; t_j, \mathbf{x}_j) = \mathbf{x}_{j+1}$). The resulting minimization problem is solved using a standard sequential quadratic program (SQP).

V. Indirect Optimization Approach

As mentioned before, the direct approach presented in the foregoing section is hard to implement on a current automotive ECU. Therefore an approach based on a simplified vehicle model will be derived in the following.
The goal is the optimization of the vehicle movement along the road. Usually one is not interested in the distance to the origin but rather in the position of the vehicle relative to the lane. As shown in [8] the vehicle motion can therefore be described directly in the so-called Frenet coordinates of the road. This facilitates the optimization compared to the optimization in global coordinates. The Frenet coordinate system is described relative to a reference curve, e.g. the center of the lane. The vehicle position is thus described by the variables $s(t)$ and its derivatives in longitudinal direction and $d(t)$ and its derivatives in lateral direction.
Hence as a fist step the vehicle states are transformed into Frenet space, see Fig. 3. The whole planning is done in these coordinates. The calculated trajectory is afterwards transformed back to vehicle coordinates and given to the underlying control. The planning algorithm will be described in the following.

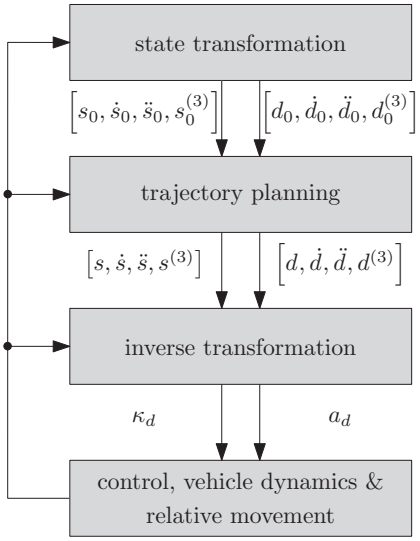

Fig. 3. Structure of the planning algorithm based on indirect optimization

A. Trajectory Planning by 6th and 7th Order Polynomials

By using the Frenet coordinates and neglecting the vehicle dynamics allows to describe the vehicle movement as an integrator system. As a virtual input the derivative of the jerk is introduced thereby. Thus the lateral and longitudinal movement of the vehicle can be described as an optimal control problem with the output $d(t) = x_1(t)$ respectively $s(t) = x_1(t)$ of a integrator system. In contrast to [8] the derivative of the jerk $x_1^{(4)}(t)$ is defined as the (virtual) input. Therefore, as will be shown in the following, polynomials of 7th order described the optimal solution. This procedure corresponds to a standard procedure according to [14].
The system dynamics are described as

$$\dot{\mathbf{x}}(t) = \begin{bmatrix} 0 & 1 & 0 & 0 \\ 0 & 0 & 1 & 0 \\ 0 & 0 & 0 & 1 \\ 0 & 0 & 0 & 0 \end{bmatrix} \mathbf{x}(t) + \begin{bmatrix} 0 \\ 0 \\ 0 \\ 1 \end{bmatrix} u(t) = \mathbf{f}(\mathbf{x}(t), u(t), t) \tag{17}$$

with $\mathbf{x^T} = [x_1, x_2, x_3, x_4]$. The cost function

$$J = h(\mathbf{x}(t_f), t_f) + \int_{t_0}^{t_f} f_0(\mathbf{x}(t), u(t), t)\mathrm{d}t \tag{18}$$

with

$$f_0(\mathbf{x}(t), u(t), t) = \frac{1}{2}u(t)^2 \tag{19}$$

is selected. The Hamiltonian

$$\mathbf{H}(\mathbf{x}(t), u(t), \boldsymbol{\lambda}(t), t) = -f_0(\mathbf{x}(t), u(t), t) + \boldsymbol{\lambda}^T \mathbf{f}(\mathbf{x}(t), u(t), t) \tag{20}$$

and the control equation $\left(\frac{\partial \mathbf{H}}{\partial u} = 0\right)$ give us

$$u = \lambda_4. \tag{21}$$

The adjoint differential equation

$$\dot{\boldsymbol{\lambda}} = -\frac{\partial \mathbf{H}}{\partial \mathbf{x}} \tag{22}$$

results to

$$\begin{pmatrix} \dot{\lambda}_1 \\ \dot{\lambda}_2 \\ \dot{\lambda}_3 \\ \dot{\lambda}_4 \end{pmatrix} = \begin{pmatrix} 0 \\ -\lambda_1 \\ -\lambda_2 \\ -\lambda_3 \end{pmatrix}. \tag{23}$$

With $\lambda_4 = u = \dot{x}_4$, (23) can be combined to

$$\begin{pmatrix} x_1 \\ x_2 \\ x_3 \\ x_4 \\ \lambda_4 \\ \lambda_3 \\ \lambda_2 \\ \lambda_1 \end{pmatrix} = \begin{pmatrix} 1 & t & t^2 & t^3 & t^4 & t^5 & t^6 & t^7 \\ 0 & 1 & 2t & 3t^2 & 4t^3 & 5t^4 & 6t^5 & 7t^6 \\ 0 & 0 & 2 & 6t & 12t^2 & 20t^3 & 30t^4 & 42t^5 \\ 0 & 0 & 0 & 6 & 24t & 60t^2 & 120t^3 & 210t^4 \\ 0 & 0 & 0 & 0 & 24 & 120t & 360t^2 & 840t^3 \\ 0 & 0 & 0 & 0 & 0 & -120 & -720t & -2520t^2 \\ 0 & 0 & 0 & 0 & 0 & 0 & 720 & 5040t \\ 0 & 0 & 0 & 0 & 0 & 0 & 0 & -5040 \end{pmatrix} \begin{pmatrix} c_0 \\ c_1 \\ c_2 \\ c_3 \\ c_4 \\ c_5 \\ c_6 \\ c_7 \end{pmatrix} \tag{24}$$

This can be transformed to

$$\mathbf{x}(t) = \underbrace{\begin{pmatrix} 1 & t & t^2 & t^3 \\ 0 & 1 & 2t & 3t^2 \\ 0 & 0 & 2 & 6t \\ 0 & 0 & 0 & 6 \end{pmatrix}}_{=:\mathbf{M}_1(t)} \mathbf{c}_{0123} + \underbrace{\begin{pmatrix} t^4 & t^5 & t^6 & t^7 \\ 4t^3 & 5t^4 & 6t^5 & 7t^6 \\ 12t^2 & 20t^3 & 30t^4 & 42t^5 \\ 24t & 60t^2 & 120t^3 & 210t^4 \end{pmatrix}}_{=:\mathbf{M}_2(t)} \mathbf{c}_{4567}. \tag{25}$$

The parameters $\mathbf{c}_{0123}^T = [c_0, ..., c_3]$ result from the initial conditions

$$\mathbf{c}_{0123} = \mathbf{M}_1^{-1}(0)\, \mathbf{x}_0 \tag{26}$$

and the parameters $\mathbf{c}_{4567}^T = [c_4, ..., c_7]$ from the not yet defined final state

$$\mathbf{c}_{4567} = \mathbf{M}_2^{-1}(t_f) \left(\mathbf{x}(t_f) - \mathbf{M}_1(t_f)\, \mathbf{c}_{0123}\right). \tag{27}$$

The optimization problem is now to determine the final time t_f and the final state $\mathbf{x}(t_f)$.
Similarly to [8] the final state is defined relative to the

reference trajectory $x_{ref}(t)$. Deviations from this trajectory will be penalized in the cost function with

$$h(\mathbf{x}(t_f), t_f) = k_t t_f + \frac{1}{2} k_x \left(x_1(t_f) - x_{ref}(t_f)\right)^2. \quad (28)$$

For driving a car we are not interested in any given final state but rather in results parallel to a given reference. This represents a target manifold with respect to the reference trajectory. The first, second and third derivative correspond to the reference trajectory and thus

$$\mathbf{z}(\mathbf{x}(t_f)) = \begin{pmatrix} x_2(t) - \dot{x}_{ref}(t) \\ x_3(t) - \ddot{x}_{ref}(t) \\ x_4(t) - x^{(3)}_{ref}(t) \end{pmatrix}_{t_f} = \mathbf{0}. \quad (29)$$

The transversality equation could now be solved, resulting in a polynomial of the optimal final time t_f. Its roots represent the optimal solution in terms of the selected cost function. As the constraints still have to be taken into account anyway, the proposed procedure of [2] is applied to determine the optimal time and final state: A set of trajectories is calculated in discrete space and their cost functions (18) are compared. Fig. 4 illustrates the procedure. The thick gray line depicts the reference trajectory. The thinner gray lines are sampled offsets. The blue lines are the calculated trajectories and in green the optimal one according to the cost function. In some

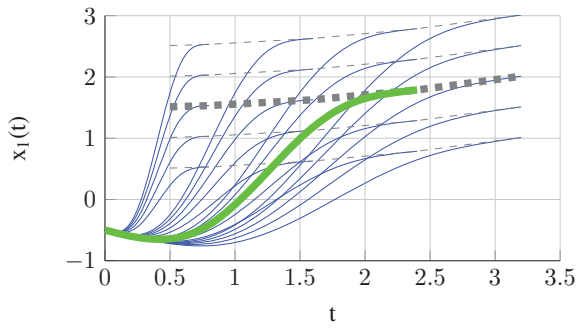

Fig. 4. Principle of discretization according to [2]: Blue the planned trajectories, green optimal in terms of cost function and gray dashed reference

cases it's not necessary to reach a defined position but only a certain speed. In this case the optimal trajectory leading from an initial state $\mathbf{x}_0$ to a final state $\mathbf{x}_f$ is defined by a polynomial of 6th order. The proof is similar to the previous one, except for the additional transversality equation $\lambda_1 = -\frac{\partial h}{\partial x} = 0$, which leads to $c_7 = 0$ [2].

B. Combined Longitudinal and Lateral Trajectory Optimization

In order to guide a vehicle along a street, longitudinal and lateral trajectories are necessary. The previous derivations will be used for the optimization of the longitudinal and lateral trajectories. Thus the whole planning consists of three steps:

1) calculating a set of longitudinal and lateral trajectories with different final times and different final states (relative to the reference line) according to the previous section
2) combining each lateral with each longitudinal trajectory and calculating its cost function
3) checking the best trajectory set for compliance with the restrictions

The first step is done by using polynomials of 7th order in lateral direction. In longitudinal direction polynomials of 6th or 7th order are used depending on the given reference. As a lateral reference serves for example the center line of the road. According to the previous explained optimal problem the cost function has to be defined. For the lateral trajectory the cost function respects the integral over the 4th derivative according to (18) and (19). In addition the deviation of the final state from the reference trajectory and the final time t_f are weighted (see (28)):

$$J_d = \frac{1}{2} \int_{t_0}^{t_f} \left(d^{(4)}(t)\right)^2 \mathrm{d}t + k_d \left(d_{ref} - d(t_f)\right)^2 + k_{t,d}\, t_f \quad (30)$$

With the weighting factors k_d and $k_{t,d}$ the characteristic of the trajectory can be parameterized.
For the optimization of the longitudinal movement, a distinction between a position and velocity planning is done similar to [8]. The position planning is carried out with 7th order polynomials and therefore considers the integral of the fourth derivative of s in the cost function:

$$J_s = \frac{1}{2} \int_{t_0}^{t_f} \left(s^{(4)}(t)\right)^2 \mathrm{d}t + k_s (s_{ref} - s(t_f))^2 + k_{t,s}\, t_f \quad (31)$$

In addition, the final time t_f and the deviation from the reference position s_{ref} are weighted. If only a certain speed $\dot{s}_{ref}$ shall be reached (without desired reference position) one can use 6th order polynomials and evaluate the costs with the following cost function:

$$J_{\dot{s}} = \frac{1}{2} \int_{t_0}^{t_f} \left(s^{(4)}(t)\right)^2 \mathrm{d}t + k_{\dot{s}} (\dot{s}_{ref} - \dot{s}(t_f))^2 + k_{t\dot{s}}\, t_f \quad (32)$$

As written before each lateral trajectory is combined with each longitudinal trajectory and thus the whole cost functions is given as

$$J = J_d + J_s \text{ or } J_d + J_{\dot{s}}. \quad (33)$$

The best trajectory according to this cost function is now checked for compliance with the restrictions given

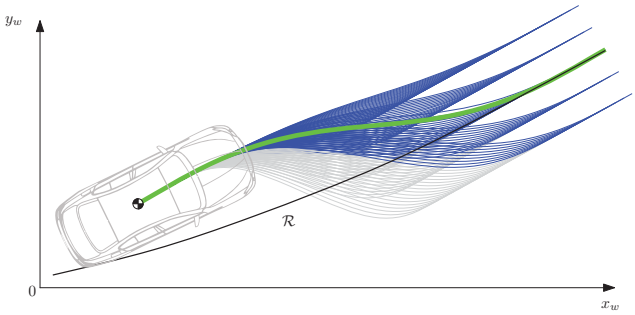

Fig. 5. Example of a set of planned trajectories leading the vehicle back to the reference $\mathcal{R}$: the optimal trajectory in green, the valid ones in blue and the invalid ones in gray

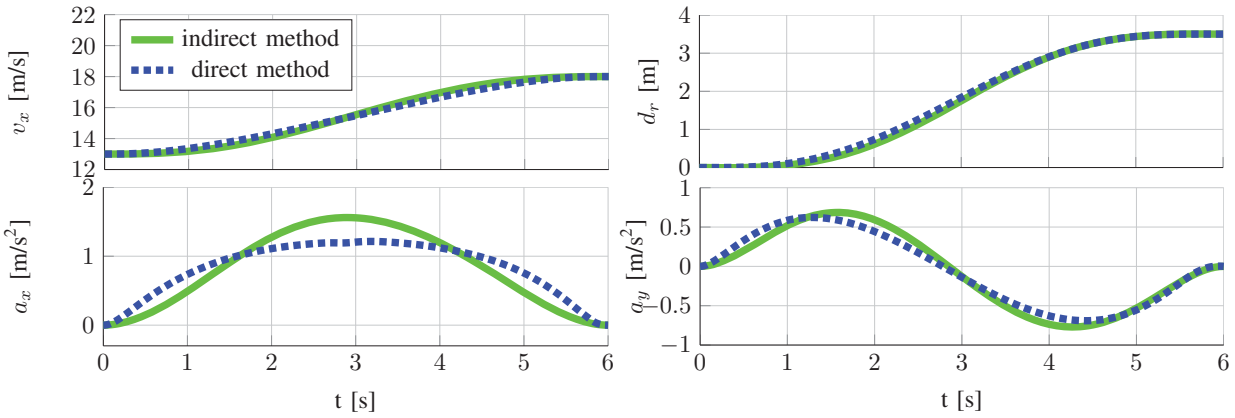

Fig. 6. Comparison of the overtaking maneuver. Green the trajectories of the indirect optimization and blue dotted the direct optimization's trajectories

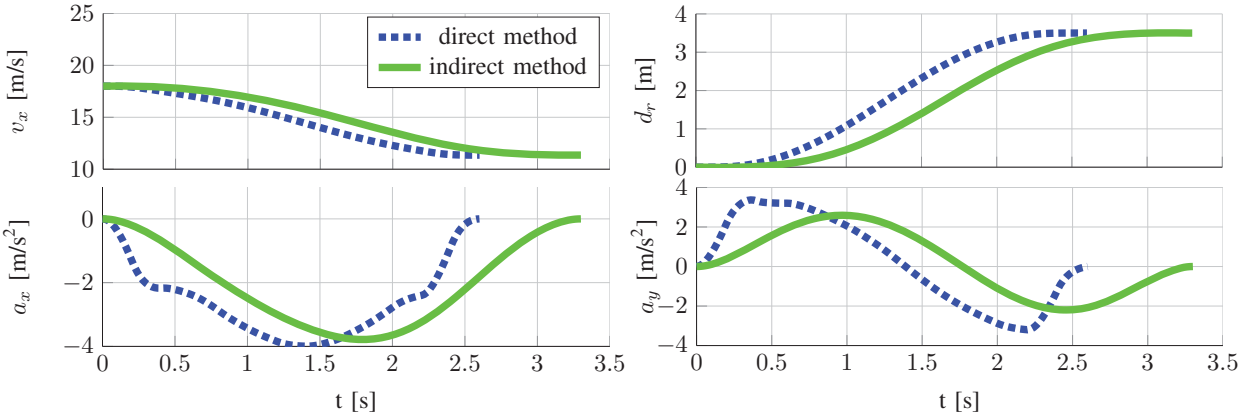

Fig. 7. Comparison of the evasion maneuver. Green the trajectories of the indirect optimization and blue dotted the direct optimization's trajectories

in Section IV. If it satisfies the constraints it is selected. Otherwise the next best trajectory is selected that complies with the constraints. Unlike [8] the restriction check isn't performed in global coordinates but within the Frenet space. The selected trajectory is transformed back to world coordinates to give it to the underlying control and actuators. Thereby the vehicle dynamics have to be considered (see for example [15]).

Fig. 5 shows the resulting trajectory for guiding a vehicle back to the reference (green line) with this approach. The blue lines depict the valid and the gray lines the invalid trajectories.

VI. Comparison of the Approaches

Both algorithms are now evaluated. As the approaches are to be applied both for comfort as well as emergency situations, two representative maneuvers are selected:

- a comfortable overtaking maneuver (changing lane and accelerating),
- an emergency braking with evasion.

In both situations a friction coefficient of 0.4 is assumed. Actuator saturations are inactive for reasons of simplicity. Fig. 6 shows the resulting accelerations for the overtaking maneuver. Both approaches calculate trajectories that do not run in the limit by the friction coefficient. It is noteworthy that both algorithms calculate trajectories with a slow slope. With the polynomial approach this is possible because 7th order polynomials are used instead of 5th order polynomials [2].

At the emergency maneuver (Fig. 7), the results of the approaches are different. Due to the limited friction the polynomial approach has to take a slower trajectory than the cost-function would suggest. The direct approach, however, can take into account this limitation directly. Thus, the resulting acceleration vector doesn't lie within the traction ellipse but exactly on its boundary (see Fig. 8). Therefore the direct approach saves time leading to a faster stopping of the car.

In summary, the resulting trajectories of both approach are quite similar in usual driving situations. Notably this is achieved in the indirect optimization without using a exact model of the vehicle dynamics. In situations where the optimization restrictions are active the direct optimization shows its advantages and can calculate trajectories leading faster to the reference compared to the indirect approach.

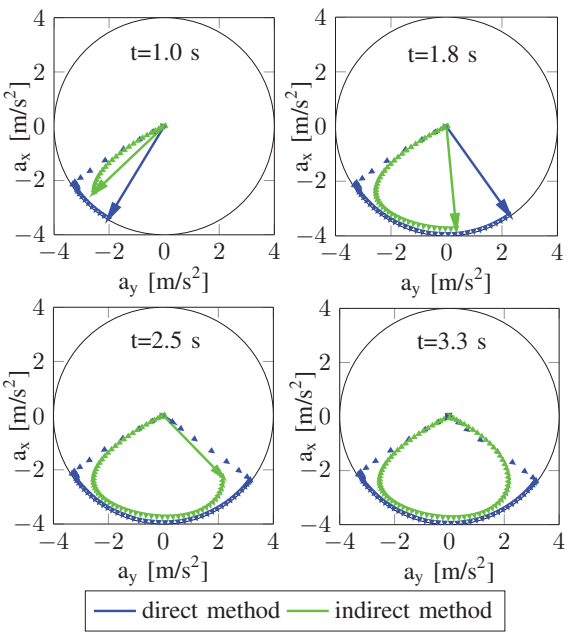

Fig. 8. Kamm's circle for the evasion maneuver

VII. Conclusion

The planning of a trajectory that takes into account all relevant constraints is necessary for future driver assistance systems. Therefore within this work two approaches for optimizing a trajectory are presented. The first one is based on direct optimization and a exact vehicle model. In contrast the second one is based on indirect optimization and a very simplified vehicle model. For usual driving situations (like overtaking) both show similar results. In situations where constraints, like actuator saturations or limited traction, are active the direct optimization saves time by directly considering the constraints within the optimization. The indirect approach however has the big advantage of being realizable on a current ECU and convergence is guaranteed as was shown.

Appendix A
Single-Track Model

The equations of the single-track model [5] results from equilibrium of forces in lateral direction and longitudinal direction and the moment equilibrium (see Fig. 9) and results in the state equations [16]

$$\dot{v} = \left(\frac{1}{m}(F_{sf}\sin(\beta-\delta) + F_{lf}\cos(\beta-\delta) + F_{sr}\sin\beta + F_{lr}\cos\beta\right) \tag{34}$$

$$\dot{\beta} = -\dot{\psi} + \frac{1}{mv}\left(F_{sf}\cos(\beta-\delta) - F_{lf}\sin(\beta-\delta) + F_{sr}\cos\beta - F_{lr}\sin\beta\right) \tag{35}$$

$$\ddot{\psi} = \frac{1}{J}\left(l_f(F_{sf}\cos\delta + F_{lf}\sin\delta) - l_r F_{sr}\right) \tag{36}$$

m describes the vehicle mass and J the moment of inertia with respect to the yaw axis at the center of gravity (COG). The distances between the COG and the front and rear axle are referred as l_f and l_r. The wheelbase results as $l = l_r + l_f$. F_{si} describes the side forces at each wheel and F_{li} the longitudinal forces. The tire force characteristic is described as proposed

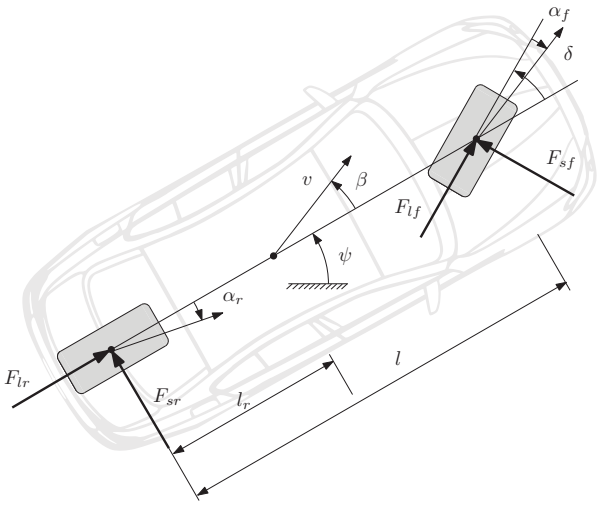

Fig. 9. Single-track model

by [17]. Accordingly, the tire forces arise as a function of the combined lateral and longitudinal slip. The force $\mathbf{F}_i = [F_{li} F_{si}]^T$ can be calculated by a nonlinear Pacejka tire model:

$$\mathbf{F}_i = A_i \sin\left(C_i \arctan\left(B_i \frac{||\mathbf{s}_i||}{\mu_i}\right)\right)\frac{1}{||\mathbf{s}_i||}\mathbf{s}_i \tag{37}$$

with the tire parameters $A_i > 0$, $B_i > 0$, $C_i > 1$. The tire slip s_i is regarded as a vector given by the relative velocity of the tire belt against the roadway caused the wheel contact [17]:

$$\mathbf{s}_i = -\frac{(\mathbf{v}_{ui} + \mathbf{v}_i)}{||\mathbf{v}_i||} \text{ with } \mathbf{v}_{ui} = -r_i\omega_i\left[\cos\delta_i \sin\delta_i\right]^T. \tag{38}$$

$\mathbf{v}_i = [v_{xi}\, v_{yi}]^T$ describes the velocity of the wheel center and can be calculated as

$$\mathbf{v}_f = \begin{pmatrix} v & 0 & 0 \\ 0 & l_f & v \end{pmatrix}\begin{pmatrix} \cos\beta \\ \dot{\psi} \\ \sin\beta \end{pmatrix} \tag{39}$$

$$\mathbf{v}_r = \begin{pmatrix} v & 0 & 0 \\ 0 & -l_r & v \end{pmatrix}\begin{pmatrix} \cos\beta \\ \dot{\psi} \\ \sin\beta \end{pmatrix} \tag{40}$$

The wheel speed ω_i results from the differential equation at the wheel

$$J_{w,i}\,\dot{\omega}_i = T_{w,i} - F_{l,i} r - F_r r \tag{41}$$

with

- $T_{w,i}$: wheel torque,
- F_r: wheel disturbance,
- $J_{w,i}$: inertia of the wheel.

REFERENCES

[1] R. Attia, R. Orjuela, and M. Basset, "Coupled longitudinal and lateral control strategy improving lateral stability for autonomous vehicle," in *American Control Conference (ACC), 2012*. IEEE, 2012, pp. 6509–6514.

[2] M. Werling and D. Liccardo, "Automatic collision avoidance using model-predictive online optimization," in *Decision and Control (CDC), 2012 IEEE 51st Annual Conference on*. IEEE, 2012, pp. 6309–6314.

[3] Y. Gao, A. Gray, J. Frasch, T. Lin, E. Tseng, J. Hedrick, and F. Borrelli, "Spatial predictive control for agile semi-autonomous ground vehicles," in *Proceedings of the 11th International Symposium on Advanced Vehicle Control*, 2012.

[4] M. Werling, J. Ziegler, S. Kammel, and S. Thrun, "Optimal trajectory generation for dynamic street scenarios in a frenet frame," in *IEEE International Conference on Robotics and Automation (ICRA)*. IEEE, 2010, pp. 987–993.

[5] P. Riekert and T.-E. Schunck, "Zur Fahrmechanik des gummibereiften Kraftfahrzeugs," *Ingenieur-Archiv*, vol. 11, no. 3, pp. 210–224, 1940.

[6] M. Walter, N. Nitzsche, D. Odenthal, and S. Müller, "Lateral vehicle guidance control for autonomous and cooperative driving," in *Proc. European Control Conference*. European Control Conference, 2014, pp. 2667–2672.

[7] M. Risch, "Der kamm'sche kreis-wie stark kann man beim kurvenfahren bremsen," *Praxis der Naturwissenschaften-Physik*, no. 5/51, pp. 7–12, 2002.

[8] M. Werling, S. Kammel, J. Ziegler, and L. Gröll, "Optimal trajectories for time-critical street scenarios using discretized terminal manifolds," *The International Journal of Robotics Research*, vol. 31, no. 3, pp. 346–359, 2012.

[9] D. Althoff, M. Buss, A. Lawitzky, M. Werling, and D. Wollherr, "On-line trajectory generation for safe and optimal vehicle motion planning," in *Autonomous Mobile Systems 2012*. Springer, 2012, pp. 99–107.

[10] I. Papadimitriou and M. Tomizuka, "Fast lane changing computations using polynomials," in *Proceedings of the American Control Conference*, vol. 1. IEEE, 2003, pp. 48–53.

[11] J. Ziegler and C. Stiller, "Fast collision checking for intelligent vehicle motion planning," in *2010 IEEE Intelligent Vehicles Symposium (IV)*. IEEE, 2010, pp. 518–522.

[12] M. Papageorgiou, *Optimierung: statische, dynamische, stochastische Verfahren*. Springer DE, 2012.

[13] H. G. Bock and K.-J. Plitt, "A multiple shooting algorithm for direct solution of optimal control problems," 1983.

[14] O. Föllinger and G. Roppenecker, *Optimale Regelung und Steuerung*, 1994.

[15] C. Rathgeber, F. Winkler, D. Odenthal, and S. Müller, "Lateral trajectory tracking control for autonomous vehicles," in *Proc. European Control Conference*. European Control Conference, 2014, pp. 1024–1029.

[16] S. Fuchshumer, "Algebraic linear identification, modelling, and applications of flatness-based control," Ph.D. dissertation, 2005.

[17] R. Orend, "Modelling and control of a vehicle with single-wheel chassis actuators," in *Proceedings of the 16th IFAC World Congress, Prague*, 2005.